Adaptive Informative Sampling with Environment Partitioning for Heterogeneous Multi-Robot Systems

Yunfei Shi, Ning Wang*, Jianmin Zheng*, Yang Zhang*, Sha Yi, Wenhao Luo, and Katia Sycara

***Abstract*— Multi-robot systems are widely used in environmental exploration and modeling, especially in hazardous environments. However, different types of robots are limited by different mobility, battery life, sensor type, etc. Heterogeneous robot systems are able to utilize various types of robots and provide solutions where robots are able to compensate each other with their different capabilities. In this paper, we consider the problem of sampling and modeling environmental characteristics with a heterogeneous team of robots. To utilize heterogeneity of the system while remaining computationally tractable, we propose an environmental partitioning approach that leverages various robot capabilities by forming a uniformly defined heterogeneity cost space. We combine with the mixture of Gaussian Processes model-learning framework to adaptively sample and model the environment in an efficient and scalable manner. We demonstrate our algorithm in field experiments with ground and aerial vehicles.**

I. Introduction

Multi-robot systems can be widely used in complicated or dangerous tasks for humans including coverage, sampling, and exploration in an unknown environment. One important application is to monitor the thermal mapping of a wildfire-affected area, e.g., the Australian bushfire, as a substitute for human observations[1]. In these scenarios, robots are expected to explore the environment, conduct sampling surveys, and build environment models including but not limited to: thermal, humidity, radio strength, etc. The problem of efficiently navigating robots to best construct environmental models is referred to as *adaptive sampling*[2], or *informative sampling*[3]. Multi-robot systems, by their distributed nature, can perform sampling tasks in parallel, which greatly increase the efficiency, adaptation, and performance.

Many of the state-of-the-art approaches related to this topic are developed based on multi-robot systems with identically designed robots, namely homogeneous multi-robot systems (e.g. [2], [3]). Although these systems are favored for simplicity in implementation and scalability, introducing heterogeneity into the system grants a better balance of cost, capability, and efficiency when conducting informative sampling [4]. Heterogeneity helps compensate for the inherent limitations of each type of robots and allows them to develop proficiencies in different aspects of the task [4]. For example, a homogeneous system with unmanned ground vehicles (UGVs) cannot utilize useful samples above bushes or rocks due to the limited reachability. Introducing unmanned aerial vehicles (UAVs) into the system helps overcome mobility constraints. Likewise, UAV's deficiency in its average battery life is counterbalanced by the UGVs continuing the sampling task while the UAVs are temporarily down for recharging.

Heterogeneity yet brings more concerns in robot coordination. It is challenging to effectively coordinate robot capabilities as they vary in characteristics and influences towards robot task performance. Some of those are complimentary, while others may result in conflicting task assignment decisions. For instance, UAV is encouraged to cover distant areas due to its agility, whereas its critical battery life constrains the range UAV can travel. The number of capabilities that need to be considered in coordination increases drastically when scaling up the system with more types of robots.

We address the heterogeneous coordination problem through a task region partitioning with high-dimensional heterogeneity cost space that captures the multifaceted capabilities of the robot team. This formulation allows the heterogeneity constraints to be imposed during task assignments, and multiple criteria can easily be incorporated by increasing the dimension of the cost space. To the best of our knowledge, our method is the first generalized framework supporting multiple heterogeneity criteria for multi-robot informative sampling.

The contribution of this paper lies in three aspects. First, we propose a novel heterogeneous environment partitioning approach that effectively leverages the capability diversity by reforming the partitioning problem in a uniformly defined heterogeneity cost space. Second, we present a system architecture for heterogeneous multi-robot informative sampling with a modularized design that allows for flexible scale-ups and extensions in both robot characteristics and team size. Third, we encapsulate our approaches into an open-source toolbox that can be easily deployed to different multi-robot sampling systems and tested it with real robots.[2]

This paper is organized as follows: we discuss the related works on multi-robot informative sampling in section II, followed by a problem overview in section III, and our approach in section IV. In section V, we evaluate our approach in both simulation and real-robot deployment. Finally, section VI concludes the paper with discussion and future works.

This work was funded by the AFOSR FA9550-18-1-0097, FA9550-1-15-0442 and Department of Agriculture (DOA) 2017-7600-726152.

[1] The authors are with the Robotics Institute at Carnegie Mellon University, Pittsburgh, PA 15213, USA., {yunfeis, ningwang, jianminz, yangzha4}@alumni.cmu.edu, {shayi, wenhao, katia}@cs.cmu.edu

* Equal Contribution

[2] Code is available at https://github.com/yangggzhang/Heterogeneous-Multi-Robot-Adaptive-Sampling

II. Related Works

The general problem of adaptive informative sampling has been widely studied in the field of robotics. Manjanna and Dudek [5] formulates the problem as a Markov Decision Process and solves the optimal policy using value iteration. In this formulation, the implicit reward function needs to be appropriately designed for different tasks. The work [6] by Kemna et al. uses single-GP regression to model the survey environment, and greedily selects the point with globally highest posterior entropy as the next sampling location. Luo and Sycara propose an informative sampling paradigm with the mixture of GPs model [7] that can more accurately predict distribution with multiple distinctive components. This method selects the next sampling points by utilizing the Gaussian Process Upper Confidence Bound (GP-UCB) [8] to optimize an information-theoretic criterion defined by the model parameters. Our method extends Luo and Sycara's informative sampling paradigm [7] with a novel environment partitioning approach that accounts for the heterogeneity of multi-robot systems with different types of robots.

Most of the state-of-the-art approaches utilize Voronoi partitioning to reduce the overlap of actions and increase sampling efficiency [2] [9] [10]. Kemna et al. [2] deploy dynamic Voronoi partitioning based on Euclidean distance in a communication-constrained multi-robot system. Similar to our method, the Voronoi partitions are recalculated during the sampling process. The work [11] by Cortes considers the possibility of an extra area constraint in normal Voronoi partitioning. This method formulates the problem as a constrained optimization problem that creates a mapping from the area constraint to weights associated with Voronoi cells and uses the weighted Voronoi partitioning to ensure the fulfillment of the constraint. Similarly, [12] solves a partitioning optimization with a congestion heuristic to enforce the collision-free constraint between robots of different sizes. These approaches are limited to regular partitioning based on Euclidean distance or with extra constraints that require customized formulations. Our method defines a unified formulation, a heterogeneity cost space, that can easily incorporate multiple constraints and heuristics, which is usually desired in heterogeneous multi-robot systems.

An approach of applying the heterogeneous multi-robot system in water sampling is presented by Manjanna et al. in [13]. The paper proposes a system of heterogeneous robots with different functionalities. The two robot boats were assigned with different tasks of exploration and physical sampling, instead of increasing efficiency and quality of one task using different capabilities of heterogeneous robots. Praneel et al. [14] developed a hierarchical system with robots of different computational capabilities completing map building and exploration tasks. However, the different mobility of robots and task region partitioning are not considered. Different from these approaches, the emphasis of our work lies in enhancing the task efficiency and generality of a multi-robot system by leveraging multiple varying capabilities of the heterogeneous robots.

III. Problem Formulation

Consider a set of n heterogeneous robots moving in a bounded environment $Q \in \mathbb{R}^2$ and assume the environment can be discretized into a set of sensing points $q \in Q$, with the position of each robot $i \in \{1,2,...,n\}$ denoted by $x_i \in Q$. The objective of heterogeneous informative sampling task is to coordinate this heterogeneous robot fleet to efficiently learn the underlying mapping $\hat{\phi}(\cdot) : Q \rightarrow \mathbb{R}_+$ from spatial location q to a scalar value of the environmental phenomenon $\phi(q)$. Very limited prior knowledge of $\phi(q)$ is assumed, yet the robot group has access to the geometry map of Q.

The entire problem can be divided into two interconnected sub-problems: environment modeling and heterogeneous informative goal selection. In modeling, we learn a model $\hat{\phi}(q)$ with samples $y_1, y_2 \dots y_n$ collected by robot $1,2 \dots n$. The sample collected by robot i at location q_i is $y_i = \phi(q_i) + \varepsilon$ which is a combination of truth phenomenon value at this location $\phi(q_i)$ and white noise ε. This model provides the informativeness over the environment, which is used in heterogeneous informative goal selection.

In heterogeneous informative goal selection, the objective is to identify a new sensing location q_i for robot i that can best improve the learned model $\hat{\phi}(q)$ while considering all the heterogeneous capabilities and constrains of robots.

In order to guarantee convergence and reducing the repetitive work as well as robot interference, we first partition the 2D environment, i.e. all sensing points $\forall q \in Q$, into n cells $V_i, i \in \{1,2,..n\}$ with a cost $L(q)$ of robots that numerically reflects their constrains and capabilities such that locations with lowest cost for robot i to explore are within $V_i = \left\{ q \in Q \| L(q_i) \leq L(q_j), \forall j \neq i \right\}$.

The goal location can be determined by solving the local optimization problem of finding $q^* \in V_i$ that maximizes the informativeness $I(q_i) \in \mathbb{R}_+$ which reflects the ability to improve the model $q_i^* = \text{argmax}_{q \in V_i} I(q_i)$. Therefore, the overall objective is to coordinate heterogeneous robots to navigate to locations that utilize heterogeneous abilities of robots and best describe the environmental model in order to learn the model $\hat{\phi}(q)$ efficiently.

IV. Approach

A. System Overview

As is illustrated in Figure 1, the system is modular-designed with a scalable number of robots and centralized to a *master computer* that processes all the samples $Y = \{y_1, y_2, ..., y_n\}$ to build the environment model $\hat{\phi}(q)$ and is responsible to send the target positions q_i to robot i. Robots contribute to the heterogeneous mobility to the system and report environment samples back to the *master computer*.

The *master computer* reads in and stores the geometric map of the area of interest Q. Given the geometric map, the *master computer* initializes a global temperature distribution model $\hat{\phi}(q)$ and keeps updating this model in real-time after receiving each sample y_i from the heterogeneous agent robot i. Once $\hat{\phi}(q)$ is updated with sample y_i, the *master computer* selects and assigns the next interest point q_i' to robot i using

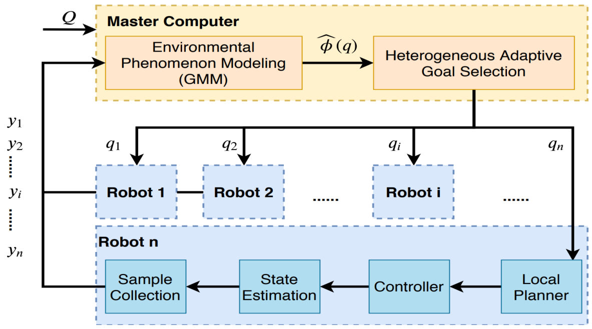

Fig. 1: The architecture of the proposed heterogeneous multi-robot sampling system. The *master computer* consists of the Mixture of Gaussian Modeling (described in section IV-B) to build the environmental model $\hat{\phi}(q)$ as well as an Heterogeneous Informative Goal Selection algorithm (described in section IV-C) that allocates sample location q_i to different robot i based on their mobility. Robot i locally process the way-point navigation control loop to achieve the target pose q_i sent from the *master computer* and report new measurement sample y_i back to the *master computer*.

the Heterogeneous Informative Goal Selection algorithm (described in section IV-C).

Agent *robot*s are deployed to the bounded area of interest Q and each robot i stores a separate geometric map of area Q in its local planner. Robot i is equipped with localization sensors and used wireless LAN to communicate with the *master computer*. During the sampling process, robot i requests and receives a target pose q_i from the *master computer* with $q_i \in Q$ and processes the navigation control loop to archive the target pose. If the way-point navigation succeed within the user-defined sampling execution period t_{samp}, robot i will report a new measurement sample y_i paired with the location q_i back to *master computer*. Otherwise, robot i will report a failure of navigation to *master computer* so that the feasibility of robot i at q_i can be updated. The entire process is running on-line and the goal of the system is to reach the convergence between the model $\hat{\phi}(q)$ and the true environmental phenomenon $\phi(q)$.

B. Mixture of Gaussian Modeling

In this section, we briefly summarize the modeling algorithm [15], [7] adopted in our approach. Due to the decentralized nature of the multi-robot sampling task given the robots spreading out over the surveyed area, we utilize a mixture of Gaussian Processes (GP) model to estimate the underlying data distribution. The mixture of GPs model [16] is a parametric probability density function defined as a linear combination of multiple GPs, which makes it ideal for handling distributions with multiple components [17].

In our problem, we assume the underlying data distribution to be investigated can be modeled by a mixture of m GPs $\{GP_1, \dots, GP_m\}$, where we assume each local GP is learned by each robot. For any point in the environment $q \in Q$, we define the probability of q being best described by the GP learned by the robot i as $P(z(q) = i)$. Then, we yield a mixture of GP models as a linear combination of $\{GP_1, \dots, GP_m\}$, weighted by the $P(z(q) = i)$ at any location $q \in Q$. The model is defined through the mean $\mu^*_{q|\tilde{V},\mathbf{Y}}$ and variance $\sigma^{*2}_{q|\tilde{V},\mathbf{Y}}$.

$$\mu^*_{q|\tilde{V},\mathbf{Y}} = \sum_{i=1}^{n} P(z(q) = i) \cdot \mu_{q|\tilde{V}_i,\mathbf{y}_i} \tag{1}$$

$$\sigma^{*2}_{q|\tilde{V},\mathbf{Y}} = \sum_{i=1}^{n} P(z(q) = i) \cdot (\sigma^2_{q|\tilde{V}_i,\mathbf{y}_i} + (\mu_{q|\tilde{V}_i,\mathbf{y}_i} - \mu^*_{q|\tilde{V},\mathbf{Y}})^2) \tag{2}$$

where $\{\tilde{V}_i, \mathbf{y}_i\}$ denotes the set of samples collected within the Voronoi partition of ith robot $\tilde{V}_i = [q^i_1, \dots, q^i_{N_i}]^T$ with data values $\mathbf{y}_i = [y^i_1, \dots, y^i_{N_i}]^T$. $\{\tilde{V}, \mathbf{Y}\}$ represents the union set of samples of value $\mathbf{Y} = \{\mathbf{y}_1, \dots, \mathbf{y_n}\}$ collected by all robots in their assigned Voronoi cells $\tilde{V} = \{\tilde{V}_1, \dots, \tilde{V}_n\}$.

Different from single-GP, we cannot simply apply Maximum Likelihood on the mixture of GPs to estimate the value of parameters, due to the lack of knowledge about the underlying weight distribution. The Expectation-Maximization (EM) algorithm [18] has been extensively used as a maximum likelihood estimation for probabilistic model parameters with hidden variables. The EM algorithm is an iterative process with two steps. In our problem, the algorithm calculates the weight distribution in the expectation step (E-Step) and then updates the parameters of local GPs with the estimated weight distribution in the maximization step (M-Step). Prior to the initial iteration, the weight distribution for any arbitrary query data point q_a is initialized to

$$P(z(q_a) = i) \approx \begin{cases} 1 & \text{if} \quad q_a \in \tilde{V}_i \\ 0 & \text{Otherwise} \end{cases} \quad \forall i = 1, \dots, n \tag{3}$$

E-Step. The algorithm updates the weight probability $P(z(q_a) = i)$ of every query point q_a for every GP model GP_i based on previous estimation. We borrow the notation $\mathcal{N}_i(q_a)$ from [7] to represent the probability of observing q_a with the local GP GP_i. Then, the weight probability can be calculated as follows.

$$P(z(q_a) = i) := \frac{P(z(q_a) = i) \cdot \mathcal{N}_i(q_a)}{\sum_{k=1}^{n} P(z(q_a) = k) \cdot \mathcal{N}_k(q_a)} \tag{4}$$

M-Step. The algorithm estimates local GP parameters after incorporating the weight probability distribution given by the E-Step. The GP parameter update rule is summarized in [15], [7] as

$$\mu_{q_{test}|\tilde{V}_i,\mathbf{y}_i} = \mathbf{k}(q_{test})^T (\mathbf{K}_{\tilde{V}_i} + \Psi^i \mathbf{I})^{-1} \mathbf{y}_i \tag{5}$$

$$\sigma^2_{q_{test}|\tilde{V}_i,\mathbf{y}_i} = ker(q_{test}, q_{test}) - \mathbf{k}(q_{test})^T (\mathbf{K}_{\tilde{\mathbf{V}}_\mathbf{i}} + \Psi^i \mathbf{I})^{-1} \cdot \mathbf{k}(q_{test}) \tag{6}$$

where the diagonal hyper-parameters in Ψ^i are $\Psi^i_{aa} = \frac{\sigma_n^2}{P(z(q_a)=i)}$. $ker(q, q')$ is the kernel function that described the correlation between two points q and q'. Following [7]'s definition, we use the same squared-exponential kernel function. $\mathbf{k}(q_{test}) = \left[ker(q^i_1, q_{test}), \dots, ker(q^i_{N_i}, q_{test})\right]^T$ is a vector that captures the correlations described by $ker(q, q')$ of all points q^i lies within the Voronoi partition of ith robot $\tilde{V}_i$ w.r.t. a testing location $q_{test} \in Q$. $\mathbf{K}_{\tilde{\mathbf{V}}_\mathbf{i}}$ denotes the positive definite symmetric kernel matrix $[ker(q, q')]_{q, q' \in \tilde{V}_i \cup q_{test}}$. The optimal hyper-parameters θ^*_i of the kernel function are obtained by maximizing of the marginal likelihood $p(\mathbf{y}_i | \tilde{V}_i, \theta_i)$ as described in [7].

C. Heterogeneous Informative Goal Selection

1) Environment Partition using Heterogeneity Primitives: Voronoi diagram is widely used [3], [7], [17] for multi-robot coordination tasks to minimize repetitive work and ensure optimal coverage and partition over the 2D Cartesian space. Each robot is associated with a Voronoi cell, and this robot has the minimum distance cost to reach any location in its cell compared with other robots. However, heterogeneity can add disturbance to the Voronoi partition. For example, a water area can fall into a ground robot's Voronoi cell in terms of 2D Euclidean distance, but the robot cannot accomplish any task within this water area. Therefore, the normal Voronoi diagram can no longer provide a reasonable partition for heterogeneous multi-robot systems. To take robotics system's heterogeneity into consideration, we define the heterogeneity space $\mathbb{H} = [h^1, \ldots, h^k] \in \mathbb{R}^k$, where each dimension $h^u, u \in \{1, 2, \ldots, k\}$ considers robots' ability for one specific heterogeneity (e.g., speed and battery life). We form the cost function of each dimension as $C^u(\delta_i^u)$, where we call δ_i^u heterogeneity primitive indicating the ability of robot i in terms of the u^{th} heterogeneity. The definition of δ_i^u is aligned with the type of cost function. Here we propose two types of cost functions:

*a) **Distance-dependent cost** C_d:* Suppose the Euclidean distance between the next targeting location and robot's current location is d. There exists a group of heterogeneities closely correlated with this distance. These properties can be either positively or negatively related to distance. For example, speed represents the distance a robot can travel within unit time, and the relationship is positive. While certain legged robots' gaits may make it very hard for them to move a short distance, then its mobility is negatively related to distance. Therefore, we formulate the cost function as

$$C_d^u(\delta_i^u, d) = \begin{cases} tanh(\delta_i^u \cdot d) & \delta_i^u \geq 0 \\ tanh(\delta_i^u \cdot d) + 1 & \delta_i^u < 0 \end{cases} \tag{7}$$

The heterogeneity primitive $\delta_i^u \in [-1, 1]$ here is a user-defined scalar. Its sign reveals the relation with distance, and its value relative to the other robot's primitive indicates the comparison of ability. For example, a faster robot should have a smaller positive speed primitive than a slower robot. This cost function can also be applied when considering battery-life, sensor coverage, etc. It worth noting that we calculate 2D distance cost using the same cost function with $\delta_i^u = 1$ for all robots.

*b) **Topography-dependent cost** C_q:* Equation (7) defines a continuous and monotonic cost function depending on distance, while topographic features can also make heterogeneous robots very different. Consider a group of robots is performing a sensing task but equipped with sensors of different operating temperatures, then the task cost heavily depends on local terrain information. In this case, we define the heterogeneity primitive $\delta_i^u \in [0, 1]$ as the cost, conditioned on the topography utility. Its user-defined value still needs to reflects the comparison in utility. For the sensory case ($u = sensory$), the topography-dependent cost function can be expressed as

$$C_q^{sensory}(\delta_i^{sensory}, q) = \begin{cases} 0 & \text{Temperature at q within } i\text{'s sensor range} \\ \delta_i^{sensory} & \text{Otherwise} \end{cases} \tag{8}$$

We concatenate the Euclidean distance and the costs in Heterogeneity space to a cost vector $\mathbf{c}_q = [C^1, C^2, \ldots, C^k]$ representing the cost to for robot i to collect a sample at point q. Each element in the cost vector is also coupled with a user-defined weight $\mathbf{w}^u \in \mathbb{R}_+$, for $u \in \{1, 2, ..., k\}$ to bias the importance among coverage or heterogeneity considerations. We compare the cost by the weighted sum and compute the final Voronoi cell for each robot

$$V_i = \left\{ q \in Q \middle| \| \sum_{u=1}^{k} \mathbf{w}^u \cdot \mathbf{c}_{q_i}^u \| \leq \| \sum_{u=1}^{k} \mathbf{w}^u \cdot \mathbf{c}_{q_j}^u \|, \forall j \neq i \right\} \tag{9}$$

2) Informative Goal Selection: The informativeness of a sample location can be defined as the ability to reduce the uncertainty of the predicted model $\hat{\phi}(q)$ as well as capture the distinctive features of the surveyed distributions. Hence we applied the Gaussian Process Upper Confidence Bound (GP-UCB) [8] strategy to balance the trade-off between exploration and exploitation. The value of informativeness at each location q is defined as [7]

$$I(q) = \mu^*_{q|\tilde{V},\mathbf{Y}} + \beta \sigma^{*2}_{q|\tilde{V},\mathbf{Y}} \tag{10}$$

where $\mu^*_{q|\tilde{V},\mathbf{Y}}$ and $\sigma^{*2}_{q|\tilde{V},\mathbf{Y}}$ are defined in (1) and (2). β is a user-specified constant to balance the trade-off of minimizing the uncertainty of the GP model and maximizing sampled value. The GP-UCB strategy we applied is sequentially selecting the most informative sample position $q_i \in V_i$ for robot i that maximizes (10) and update the GP model consequently to reach the balance. [7]

V. Experimental Results

We implemented and evaluated our system using both simulation and real robots. The codebase was built on the Robot Operating System (ROS). Our algorithm can be used for general environmental feature modeling tasks, including thermal, humidity, and radio strength, etc. However, most of these environment features are either difficult to set up and capture, or relatively constant within our limited range of testing site, we chose to conduct WiFi signal strength sampling tasks to demonstrate our approach. We collected a real-world 2D WiFi signal strength distribution dataset for the experiments. In a 9m x 14m open area, we randomly placed 2 or 3 WiFi signal generators and manually measured WiFi strength every 1 meter, resulting in 150 samples in total for each trail. We first conducted a modeling performance comparison between the mixture of GPs and the uni-modal GP. We then compared our method with informative sampling without considering robots' differences in simulation. In field experiments, we deployed a heterogeneous multi-robot system consists of one UAV and one UGV to perform the real-world task.

A. Modeling Performance Comparison

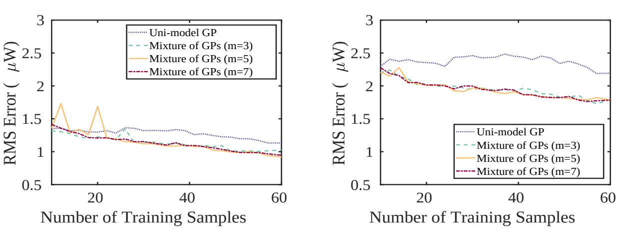

(a) 2 WiFi signal generators (b) 3 WiFi signal generators

Fig. 2: Model prediction performance comparison between the mixture of GPs with $m = 3, 5, 7$ and uni-modal GP on two real-world WiFi signal strength datasets with (a) two and (b) three WiFi signal generators. Each line represents the mean RMS error over 10 random trials.

We applied different mixture of GPs (m = 1,3,5,7) models and a uni-modal GP on two datasets, one with two (Fig.2a) and the other with three WiFi signal generators (Fig.2b). We randomly selected a certain number of training samples from the dataset and computed the predictions on all available sampling positions. We then compared the predictions with the ground truth collections to compute root-mean-square error (RMSE). The results in Fig.2 show that the mixture of GPs outperforms the uni-modal GP in both scenarios given the same number of training data, showing its greater ability to model non-trivial environmental phenomenon.

B. Simulation

We deployed three robots in the simulation: one aerial and two ground robots. The simulation field range aligned with that in our collected dataset. We randomly spawned 1 - 2 circular (0.5m radius) obstacles for each test. The ground robots need to avoid the obstacles while the aerial robot can traverse over the obstacles. We assumed each robot has optimal waypoint following control and perfect localization. All robots are using the same optimal trajectory planner, and we implemented a dynamic window approach (DWA)[19] obstacle avoidance algorithm for ground robots. All robots can measurement WiFi signals from the ground truth data with a Gaussian noise $\varepsilon \sim \mathcal{N}\left(0, 0.65^2\right)$. To provide ground-truth measurements at more locations in simulation, we interpolated the WiFi signal dataset using a 5^{th} order polynomial fit by the MATLAB Polynomial Toolbox.

The robots in our simulation are different in speed, battery life and traversability with detailed configurations listed in Table. I. The three differences come up with three heterogeneity cost functions. Speed and battery costs are distance-dependent, and their heterogeneity primitives are also listed in Table. I. We want to penalize the costs for ground robots to collect samples falling on obstacles. Then we set the topography-dependent traversal cost for ground robots to be 1 for obstacle-occupied locations and 0 otherwise. The traversal cost for the aerial robot is always 0 over the entire region. The weights for each cost are 2.0, 1.5, and 10^6 respectively, and we assigned the weight for Euclidean distance to be 1 for all tests. For the simplicity of implementation, we set a battery life as a termination threshold in ROS time.

Robot ID	Robot Type	Speed (m/s)	Battery Life (s)	Traverse Obstacle	Speed Primitive	Battery Life Primitive
1	UGV	1	200	False	1.0	0.75
2	UGV	2	200	False	0.5	0.75
3	UAV	5	25	True	0.2	1.0

TABLE I: Robot Configurations in Simulation.

We compared our algorithm with the homogeneous informative sampling method[7], the region partition of which is a normal Voronoi diagram without considering robots' differences, as shown in the leftmost plot in Figure 3. The additional speed cost considered in the Heterogeneous Partition (HP) 1 results in the fastest robot (aerial robot in green) covering more regions , but it also suffers from a shorter battery life compared to ground robots. Therefore, we want it to spend more time collecting samples instead of traveling within its short operation time. Adding the corresponding cost gives us the HP2, in which the aerial robot's region shrinks compared to the HP1. It is a wasted and dangerous move to let ground robots collect samples above obstacles, for this reason, we significantly increased the weighting factor for traversability cost. Then the obstacle falls into the aerial robot's partition even if it is a great distance away (HP3). The results in Figure 3 show that considering heterogeneity space costs would give heterogeneous multi-robot systems a more reasonable region partition.

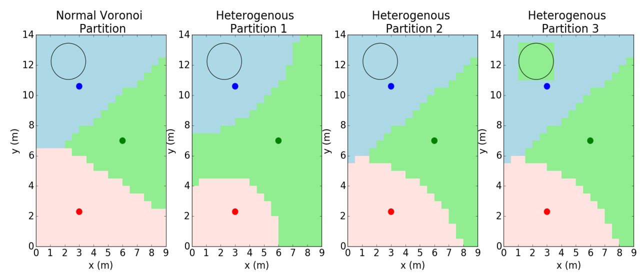

Fig. 3: The red, blue and green dots represent the current locations of the ground robot 1, 2 and the aerial robot respectively. The corresponding shallow areas are their responsible regions. The black circle denotes an obstacle that the robot 1 and 2 need to avoid. The first partition from left uses normal Voronoi Diagram; the second adds speed heterogeneity; the third adds battery life, and the last adds traversability.

We initialized the sampling tasks with six randomly selected samples. We showed our algorithm's strength over the homogeneous method in Figure 4. Our method outputs a smaller RMSE through the entire simulation. Notably, the heterogeneous RMSE dropped much faster than homogeneous RMSE with slightly more collected samples before the aerial robot stopped operation, and the convergence rates do not get closer before convergence. The final RMSE difference is also smaller than the difference during sampling. These results show our algorithm does not naively facilitate informative sampling by assigning aerial robots to obstacles but does help improving sampling efficiency and modeling accuracy. Our method outperforms the homogeneous method by giving a better convergence rate, a more accurate prediction and more sample collections for the informative sampling task. Our approach can finish tasks faster under the stopping criteria using RMSE or the number of samples when the ground truth data is not available, which is usually the case in real environment deployment.

C. Field Experiments

We deployed the heterogeneous multi-robot informative sampling system on hardware robots with one UGV (Clearpath Jackal) and one UAV (AscTec Pelican), both equipped with an RTK-GPS localize and a Panda PAU09 wireless adapter to monitor the WiFi signal strength. The experiment was conducted in a $10m \times 10m$ outdoor test field on the campus of Carnegie Mellon University. We paired

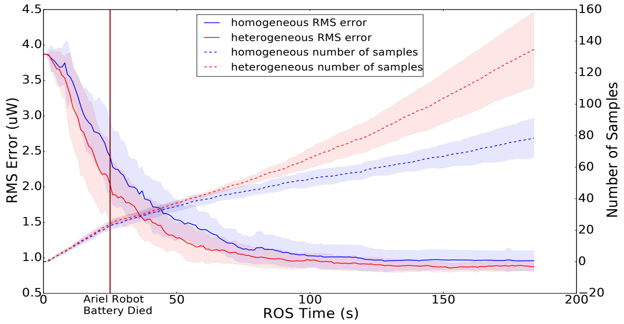

Fig. 4: Informative sampling performance comparison between heterogeneous and homogeneous multi-robot sampling algorithms. We run each algorithm on the same dataset 45 times with random robot initial locations and obstacle positions. The shallow areas represent the variance range. The red vertical line indicates the time when the aerial robot stopped operation.

three WiFi signal generators with three obstacles placed in different positions. 3 WiFi signal generators were placed above each of the obstacles. Robot agents were deployed to the test field to perform the sampling task. The UAV took samples at the same height as the UGV. We ran the experiments for 12 minutes (UAV battery life), and later manually collected 150 ground truth data. (Figure 5) resulting in an RMSE of 2.93 μW. The result is not as ideal as simulation due to difficulties in real-world operation.

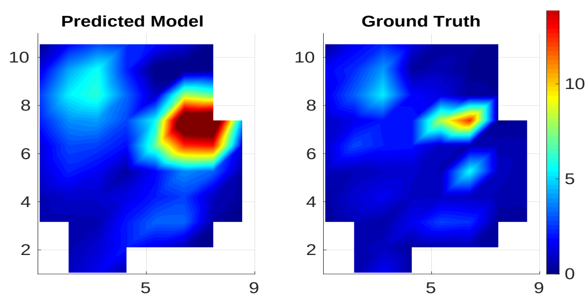

Fig. 5: Outdoor test result

VI. Conclusion

This paper presented an informative sampling approach for heterogeneous multi-robot systems to model environmental phenomena. By partitioning task regions with uniformly defined high-dimensional heterogeneity cost and applying the GP-UCB algorithm, we are able to leverage diverse robot capabilities and increase the informativeness of samples to extensively improve the sampling efficiency. The high dimensional heterogeneity cost space we defined joins different heterogeneity properties on the same scale and provides great scalability in terms of the number of heterogeneity primitives considered. This novel approach also provides the foundation of our modular-designed heterogeneous multi-robot system architecture. Besides, we used a mixture of Gaussian Processes for modeling to better capture the multi-modal distribution of real-world environmental phenomena to further improve the accuracy of the predicted model. Simulation results have shown the superiority of our algorithm compared to the previous approach of homogeneous sampling [7]. In the future, we will investigate the online heterogeneous environment partitioning with no prior knowledge of the geometry map and auto-tuning of parameters.

References

[1] T. Manderson, S. Manjanna, and G. Dudek, "Heterogeneous robot teams for informative sampling," *arXiv preprint arXiv:1906.07208*, 2019.

[2] S. Kemna, J. G. Rogers, C. Nieto-Granda, S. Young, and G. S. Sukhatme, "Multi-robot coordination through dynamic voronoi partitioning for informative adaptive sampling in communication-constrained environments," in *2017 IEEE International Conference on Robotics and Automation (ICRA)*, May 2017, pp. 2124–2130.

[3] N. Fung, J. Rogers, C. H. Nieto, H. I. Christensen, S. Kemna, and G. S. Sukhatme, "Coordinating multi-robot systems through environment partitioning for adaptive informative sampling," *International Conference on Robotics and Automation (ICRA)*, pp. 3231–3237, 2019.

[4] A. Martin, "A framework for the development of scalable heterogeneous robot teams with dynamically distributed processing," Ph.D. dissertation, University of Toronto, 2013.

[5] S. Manjanna and G. Dudek, "Data-driven selective sampling for marine vehicles using multi-scale paths," *IEEE/RSJ International Conference on Intelligent Robots and Systems (IROS)*, pp. 6111–6117, 2017.

[6] S. Kemna, D. A. Caron, and G. S. Sukhatme, "Adaptive informative sampling with autonomous underwater vehicles: Acoustic versus surface communications," in *OCEANS 2016 MTS/IEEE Monterey*, Sep. 2016, pp. 1–8.

[7] W. Luo and K. Sycara, "Adaptive sampling and online learning in multi-robot sensor coverage with mixture of gaussian processes," in *IEEE International Conference on Robotics and Automation (ICRA)*. IEEE, 2018, pp. 6359–6364.

[8] N. Srinivas, A. Krause, S. M. Kakade, and M. W. Seeger, "Information-theoretic regret bounds for gaussian process optimization in the bandit setting," *IEEE Transactions on Information Theory*, vol. 58, no. 5, pp. 3250–3265, May 2012.

[9] A. Breitenmoser, M. Schwager, J. Metzger, R. Siegwart, and D. Rus, "Voronoi coverage of non-convex environments with a group of networked robots," in *IEEE International Conference on Robotics and Automation*, May 2010, pp. 4982–4989.

[10] M. Lindhe, P. Ogren, and K. H. Johansson, "Flocking with obstacle avoidance: A new distributed coordination algorithm based on voronoi partitions," in *Proceedings of the 2005 IEEE International Conference on Robotics and Automation*, April 2005, pp. 1785–1790.

[11] J. Cortes, "Coverage optimization and spatial load balancing by robotic sensor networks," *IEEE Transactions on Automatic Control*, vol. 55, no. 3, pp. 749–754, March 2010.

[12] O. Arslan and D. E. Koditschek, "Voronoi-based coverage control of heterogeneous disk-shaped robots," in *IEEE International Conference on Robotics and Automation (ICRA)*, May 2016, pp. 4259–4266.

[13] S. Manjanna, A. Q. Li, R. N. Smith, I. M. Rekleitis, and G. Dudek, "Heterogeneous multi-robot system for exploration and strategic water sampling," *IEEE International Conference on Robotics and Automation (ICRA)*, pp. 1–8, 2018.

[14] P. Chand and D. A. Carnegie, "Mapping and exploration in a hierarchical heterogeneous multi-robot system using limited capability robots," *Robotics and autonomous Systems*, vol. 61, no. 6, pp. 565–579, 2013.

[15] C. Stachniss, C. Plagemann, and A. J. Lilienthal, "Learning gas distribution models using sparse gaussian process mixtures," *Autonomous Robots*, vol. 26, no. 2, pp. 187–202, 2009. [Online]. Available: https://doi.org/10.1007/s10514-009-9111-5

[16] V. Tresp, "Mixtures of gaussian processes," *Advances in Neural Information Processing Systems*, vol. 13, 02 2001.

[17] W. Luo, C. Nam, G. Kantor, and K. Sycara, "Distributed environmental modeling and adaptive sampling for multi-robot sensor coverage," in *Proceedings of the 18th International Conference on Autonomous Agents and MultiAgent Systems*, 2019, pp. 1488–1496.

[18] T. K. Moon, "The expectation-maximization algorithm," *IEEE Signal Processing Magazine*, vol. 13, no. 6, pp. 47–60, Nov 1996.

[19] D. Fox, W. Burgard, and S. Thrun, "The dynamic window approach to collision avoidance," *IEEE Robotics & Automation Magazine*, vol. 4, no. 1, pp. 23–33, 1997.